

# **METHODOLOGY FOR ESTIMATING SEISMIC COEFFICIENTS FOR PERFORMANCE-BASED DESIGN OF EARTH DAMS AND TALL EMBANKMENTS**

**Achilleas G. Papadimitriou**

Assistant Professor, Department of Civil Engineering,  
University of Thessaly, Greece

**George D. Bouckovalas**

Professor, Geotechnical Department, School of Civil Engineering,  
National Technical University of Athens, Greece

**Konstantinos I. Andrianopoulos**

Post-Doctoral Researcher, Geotechnical Department, School of Civil Engineering,  
National Technical University of Athens, Greece

Paper submitted for publication to *Soil Dynamics and Earthquake Engineering*

Text + 1 Table & 15 Figures

**KEYWORDS:** earthdams, earthquake, embankments, non-linear soil response,  
numerical analysis, performance-based design, pseudo-static analysis,  
sliding block, slope stability

**CONTACT ADDRESS:** Achilleas Papadimitriou  
Department of Civil Engineering  
University of Thessaly  
Pedion Areos, 38334, Volos, Greece  
Tel. +30-24210-74140  
Fax. +30-24210-74169  
Email. [apapad@civ.uth.gr](mailto:apapad@civ.uth.gr)  
Web. <http://apapad.users.uth.gr>

# METHODOLOGY FOR ESTIMATING SEISMIC COEFFICIENTS FOR PERFORMANCE-BASED DESIGN OF EARTH DAMS AND TALL EMBANKMENTS

Achilleas G. Papadimitriou<sup>1</sup>, George D. Bouckovalas<sup>2</sup>

Konstantinos I. Andrianopoulos<sup>3</sup>

## Abstract

Following an overview of pertinent literature, this paper presents a new methodology for estimating seismic coefficients for the performance-based design of earth dams and tall embankments. The methodology is based on statistical regression of (decoupled) numerical data for 1084 potential sliding masses, originating from 110 non-linear seismic response analyses of 2D cross sections with height ranging from 20 to 120m. At first, the methodology estimates the peak value of the seismic coefficient  $k_{hmax}$  as a function of: the peak ground acceleration at the free field, the predominant period of the seismic excitation, the non-linear fundamental period of dam vibration, the stiffness of the firm foundation soil or rock layer, as well as the geometrical characteristics and the location (upstream or downstream) of the potentially sliding mass. Then, it proceeds to the estimation of an effective value of the seismic coefficient  $k_{hE}$ , as a percentile of  $k_{hmax}$ , to be used with a requirement for pseudo-static factor of safety greater or equal to 1.0. The estimation of  $k_{hE}$  is based on allowable permanent down-slope deviatoric displacement and a conservative consideration of sliding block analysis.

*Keywords*— earthdams, earthquake, embankments, non-linear soil response, numerical analysis, performance-based design, pseudo-static analysis, sliding block, slope stability

---

<sup>1</sup> Assistant Professor, Department of Civil Engineering, University of Thessaly, Greece, < [apapad@civ.uth.gr](mailto:apapad@civ.uth.gr) >

<sup>2</sup> Professor, Department of Geotechnical Engineering, School of Civil Engineering, National Technical University of Athens, Greece, < [gbouck@central.ntua.gr](mailto:gbouck@central.ntua.gr) >

<sup>3</sup> Post-Doctoral Researcher, Department of Geotechnical Engineering, School of Civil Engineering, National Technical University of Athens, Greece, < [kandrian@tee.gr](mailto:kandrian@tee.gr) >

## 1. INTRODUCTION

It is well known that the assessment of seismic stability of earth structures may be performed via: (a) traditional and easy to use pseudo-static analyses, (b) a great number of available displacement-based (Newmark or sliding block) methods, and (c) dynamic stress-deformation numerical analyses. Although robust numerical analyses, i.e. method (c), are nowadays quite common, methods (a) and (b) are still the basis of engineering practice in the aseismic design of earth dams and natural slopes worldwide, at least in the preliminary design stages.

Pseudo-static analyses have the benefit of accumulated experience, reduced cost and user-friendliness, since they merely require the estimation of a Factor of Safety  $FS_d$  against seismic “*failure*” of the slopes of the earth structure. The described problem is illustrated in Fig. 1, which also depicts significant problem parameters like the peak values of the seismic acceleration at the crest,  $PGA_{crest}$ , at the outcropping (bed)rock  $PGA_{rock}$  and at the “*free-field*” of the foundation soil,  $PGA$ . The critical measure of the whole analysis is the value of the horizontal inertial force  $F_h$  that is applied at the center of gravity of the sliding mass and equals to the weight of the mass  $W$  multiplied by a dimensionless seismic coefficient  $k_h$ . At any rate, the value of  $F_h$  (and  $k_h$ ) should reflect the vibration of the sliding mass during the design earthquake, and its rational selection is therefore critical.

Given that the sliding mass is not rigid, different locations within this mass do not vibrate in phase and with the same intensity. For instance, this is especially true for deep sliding masses in tall dams where vibration is less intense deep within the dam body, as compared to its surface, and the predominant wave length  $\lambda_d$  of the seismic shear waves within the dam body is comparable to the dam height  $H$ . Therefore, the value of  $k_h$  should be related to the resultant (horizontal) acceleration time history of the sliding mass, which, in turn, has been related to the resultant (horizontal) force time history along the shear band delineating the sliding mass within the dam body. This resultant acceleration time history is generally not

equal to the acceleration time history at any standard “*reference*” location within, or in the vicinity of the dam (e.g. the “*free-field*” of the foundation soil, the outcropping bedrock, the crest of the dam or its base). On the contrary, this resultant acceleration time history is generally expected to be a function of the characteristics of the dam and the excitation, as well as the geometry of the sliding mass (Makdisi and Seed 1978), but also to be affected by whether slippage has initiated along the shear band that delineates the sliding mass within the dam body (Rathje and Bray 2000).

Overall, there are two types of numerical procedures for estimating resultant acceleration time histories (and displacements) of sliding masses, i.e. “*decoupled*” procedures where the dynamic response of the examined dam is calculated separately from possible slippage of any sliding mass within it (e.g. Makdisi and Seed 1978, Lin and Whitman 1983) and “*coupled*” procedures where the dynamic response of the sliding mass (and not the dam) is considered simultaneously to the accumulation of permanent deviatoric displacement (e.g. Kramer and Smith 1997, Rathje and Bray 2000). In any case, it becomes obvious that an accurate estimation of the resultant time history of a flexible sliding mass requires robust dynamic numerical analyses, which are demanding in software, expertise and cost, and hence beat the purpose of choosing method (a) over (c). Hence, in order to avoid such analyses, researchers and practitioners around the world have devised various empirical methods for estimating appropriate values of seismic coefficients to be used in pseudo-static analyses (e.g. USCOLD 1985, Charles et al. 1991). Andrianopoulos et al. (2012) presents a critical evaluation of such methods and shows that they generally disregard important problem parameters (e.g. dam characteristics) and may prove unconservative (e.g. for shallow sliding masses).

Yet, in all cases, the peak of the resultant acceleration time history, denoted hereafter as  $k_{hmax}$ , has never been considered an appropriate value of  $k_h$  for use in pseudo-static analyses. This is because  $k_{hmax}$  is observed momentarily and therefore an analysis using this value along with a

requirement for  $FS_d \geq 1.0$  leads to an over-conservative design. Hence, common practice dictates the use of an “*effective*” value of the seismic coefficient  $k_{hE}$  (a percentile of  $k_{hmax}$ ) in combination with the requirement for  $FS_d \geq 1.0$ , as more representative of the overall intensity of the shaking throughout its duration. This  $k_{hE}/k_{hmax}$  ratio in the literature ranges from 0.5 to 0.8, and its value has mostly been selected on the basis of experience and intuition (Papadimitriou et al. 2010). This simple method of rationalizing the design comes at the expense of generally “*small*”, but yet unknown, permanent down-slope deviatoric displacements (e.g. Hynes-Griffin and Franklin (1984) suggest that use of  $k_{hE}/k_{hmax} = 0.5$  leads to displacements less than 30cm, a value corroborated by Bozbey and Gundoglu (2011) who also showed that for PGA less than 0.5g these displacements are even less than 20cm).

Based on the above, it becomes obvious that permanent down-slope deviatoric displacements don’t directly govern, but are related to the selection of an “*effective*” seismic coefficient for the traditional pseudo-static design of earth dams and tall embankments, or method (a) above. On the contrary, nowadays, these displacements play the lead role in modern performance-based design of such structures, or method (b) above. In particular, Newmark (1965), being the pioneer of this effort, devised the rigid sliding block theory for downslope deviatoric displacement computations based on the estimation of the yield acceleration of the sliding mass  $k_y g$  (where  $g$  is the acceleration of gravity and  $k_y$  the yield seismic coefficient), via trial-and-error pseudo-static analyses for  $FS_d = 1$ . Note that this threshold value of (yield) acceleration indirectly reflects the strength of the geomaterials along the shear band and the geometry and weight of the sliding mass. According to this method, the accumulated downslope deviatoric displacements of the slopes may be obtained by double integration of the relative acceleration, i.e. of the difference between the resultant acceleration time history and the critical acceleration  $k_y g$  of the sliding mass

In Newmark’s proposition, the sliding mass was considered rigid and required case-specific

time-histories for estimating displacements. To alleviate the latter problem, many research efforts ever since have made parametric use of this basic concept for a large number of seismic recordings attempting to devise user-friendly equations and/or charts for estimating permanent down-slope displacements, given different selections of seismic motion measures (e.g. earthquake magnitude  $M$ , PGA, peak ground velocity PGV, Arias intensity, predominant  $T_e$  excitation period) and the value of the yield seismic coefficient  $k_y$  (e.g. Franklin and Chang 1977, Richards and Elms 1979, Whitman and Liao 1984, Ambraseys and Menu 1988, Cai and Bathurst 1996, Jibson 2007, Saygili and Rathje 2008, Bozbey and Gundoglu 2011). Realizing further that the rigid block assumption is potentially too crude for a deep and flexible sliding mass, many researchers went on to estimate the resultant acceleration time-history and the down-slope displacement of this sliding mass, either with “*decoupled*” (e.g. Makdisi and Seed 1978) or with “*coupled*” analyses (e.g. Rathje and Bray 2000). Again, parametric analyses for large databases of seismic recordings enabled the proposal of empirical equations and/or design charts for estimating permanent down-slope displacements using “*decoupled*” (e.g. Makdisi and Seed 1978, Bray and Rathje 1998), but mostly “*coupled*” analyses (e.g. Bray and Travarasrou 2007, Rathje and Antonakos 2011). The proposed equations and/or design charts appropriately employed seismic intensity measures related to the resultant acceleration time history of the sliding mass (e.g.  $k_{hmax}$ ), rather than the seismic excitation itself (e.g. PGA) as in rigid sliding block methods. Hence, besides the need for estimating  $k_y$  via pseudo-static analyses, some of these displacement-based methods also include procedures for estimating the peak seismic coefficient,  $k_{hmax}$ . Again, Andrianopoulos et al. (2012) performs a critical evaluation of such procedures, and shows that they may also disregard important problem parameters (e.g. reservoir impoundment, existence of berms), while, in some cases, they are cumbersome to employ since they are not stand-alone methodologies (e.g. Makdisi and Seed 1978 require the independent estimation

of  $PGA_{crest}$ ).

In conclusion, methods (a) and (b) for the seismic design of earth dams and tall embankments are, in reality, clearly interrelated. Acknowledging this fact, there are efforts in the literature lately to directly relate the appropriate selection of an “*effective*” seismic coefficient  $k_{hE}$  (for use in pseudo-static analyses) to the allowable downslope deviatoric displacement (Biondi et al. 2007, Bray and Travararou 2009, Zania et al. 2011, Bozbey and Gundogdu 2011). These efforts definitely reduce the arbitrary nature by which the  $k_{hE}/k_{max}$  ratio has been dealt with in the past. Yet, Biondi et al (2007) and Bozbey and Gundogdu (2011) deal with very specific sliding mass geometries (infinite slope, wedge in slope) that cannot cover all potential sliding masses of earthdams and tall embankments. On the other hand, Bray and Travararou (2009) propose an elegant scheme for estimating  $k_{hE}$  by considering it equal to  $k_y$  and requiring that  $FS_d = 1$  for a given level of allowable displacements. To do so they propose an equation that uses an intensity parameter that is not yet well-established in engineering practice (spectral acceleration  $S_a$  for an elongated period of the sliding mass) and is related to the seismic excitation and not the dam vibration. Finally, Zania et al (2011) propose a “*seismic coefficient spectrum*” that yields values of  $k_{hE} < k_{hmax}$  as a function of slope displacements. In concept, it is a rational approach, since it incorporates resonance and out-of-phase dam vibration effects, but their results pertain to specific sliding mass geometries and come with significant scatter due to the employed correlation to PGA, rather than  $PGA_{crest}$  (the latter is related to dam vibration, but not the former).

This paper falls within this last category of recent research efforts and aims at explicitly introducing performance-based design concepts in the well-known (to practitioners) methodology of pseudo-static analysis. It also aims to propose a stand-alone and easy-to-use method for any potential sliding mass geometry, and to take into account all important problem parameters, thus remedying the insufficiencies of existing methodologies from the

literature. To do so, it first proposes a methodology for independent estimation of the peak seismic coefficient  $k_{hmax}$  (Section 3) and then proceeds to the estimation of its “*effective*” value  $k_{hE}$  based on allowable displacements and a conservative consideration of sliding block analysis (Section 4). These tasks are enabled by statistical regression of numerical results originating from a large number of two dimensional (2D) non-linear seismic response “*decoupled*” analyses of earth dams (for actual acceleration time histories), which address parametrically the effects of all important problem parameters (Section 2). The paper ends (Section 5) with a discussion on the accuracy and the limitations of the proposed methodology.

## **2. DESCRIPTION OF NUMERICAL ANALYSES**

### **2.1 Overview**

Attempting a “*decoupled*” approach to the problem, the numerical investigation is based on a total of 110 two-dimensional (2D) seismic response analyses of earthdams that yielded results for 1084 potential sliding masses. These non-linear analyses were executed using the commercial finite difference code FLAC (Itasca, 2005), that performs integration of wave equations in the time domain. The analyses studied parametrically the effects of:

- Intensity and frequency content of the excitation ( $PGA = 0.05 - 0.5g$ ,  $T_e = 0.14 - 0.5s$ )
- Foundation conditions (shear wave velocities of the foundation soil,  $V_b = 250 - 1500m/s$ )
- Existence of (large) stabilizing berms
- Reservoir impoundment, and
- The exact geometry of the potential sliding mass



As described in Andrianopoulos et al. (2012), most of these parameters are not accounted for in existing methodologies for estimating seismic coefficients for earthdams and tall embankments. Hence, the study here focused on the effects of the foregoing parameters on three (3) fundamental aspects of seismic response of such geostructures, namely the non-linear fundamental period of dam vibration,  $T_o$ , the peak acceleration at the dam crest,  $PGA_{crest}$ , and the peak value of the seismic coefficient  $k_{hmax}$  for various sliding masses within the dam body.

In order to provide for the greatest possible applicability of the methodology, the response of four (4) cross sections was analyzed parametrically, namely cross sections of:

- $H = 20\text{m}$  (tall embankment, with base width equal to 80m)
- $H = 40\text{m}$  (rather short earth dam, with base width equal to 210m)
- $H = 80\text{m}$  (medium height earth dam, with base width equal to 415m)
- $H = 120\text{m}$  (tall earth dam, with base width equal to 615m)

The slope inclinations of the earth dams ranged from 1:2 to 1:2.5 (vertical : horizontal) in order to ensure ample static stability. In the cases of  $H = 40, 80$  and  $120\text{m}$  the earth dam possessed a clay core with slope inclinations ranging from 4:1 to 5:1, while for the case of  $H = 20\text{m}$  the embankment was considered uniform.

In order to investigate the effect of stabilizing berms on the seismic response of an earthdam, variations of the foregoing sections were also studied. These variants of dam sections possessed typical berms of height and width equal to  $H/3$  and  $2H/3$  respectively on both sides of the body of the dam, for  $H = 40$  and  $80\text{m}$ . Furthermore, in order to investigate the effect of foundation conditions on the seismic response, the same cross sections of dams were analyzed for various shear wave velocities of the foundation soil, from  $V_b = 250\text{m/s}$  up to  $1500\text{m/s}$  (the smaller value only for  $H=20\text{m}$ ). Finally, in order to investigate the effect of

reservoir impoundment on the seismic response, the same cross sections were analyzed for end of construction and steady state seepage conditions. The former conditions pertain to unsaturated geomaterials comprising the dam, while the latter to saturated upstream geomaterials and a fully impounded reservoir.

The finite difference analyses were performed with dense meshes (maximum zone dimension equal to 1/10 of the predominant shear wavelength) of large dimensions (e.g. lateral extent of at least 2H), that were equipped with proper boundary conditions (e.g. free-field lateral boundaries). The employed seismic excitations were based on recordings from actual earthquakes, with the predominant periods  $T_e$  ranging between 0.14sec and 0.50sec, i.e. covering the whole range of usually expected (at least in Southern Europe) significant periods for bedrock excitations. Further details on the numerical simulations and their results may be found in Bouckovalas et al (2009) and Andrianopoulos et al (2012).

## **2.2 Constitutive model for geomaterials**

The mechanical response under dynamic loading of the various geomaterials comprising the earthdams was simulated via the non-linear hysteretic constitutive model described below, that has been implemented as a User-Defined-Model routine by the authors. In all cases, the soil is modeled as a non-linear hysteretic material using constantly updating values of the tangential bulk  $K_t$  and shear  $G_t$  moduli. In particular, following isotropic elasticity, the  $K_t$  and  $G_t$  are interrelated via a constant elastic Poisson's ratio  $\nu$  (a model constant). Then, based on Andrianopoulos et al (2010), Andrianopoulos (2006) and Papadimitriou (1999), the non-linear hysteretic form of  $G_t$  is given the following generalized Ramberg and Osgood (1943) type of relation for monotonic and cyclic loading paths:

$$G_t = \frac{G_{\max}}{T} \quad (1)$$

$$\mathbf{T} = \left\{ \begin{array}{l} 1 + 2 \left( \frac{1}{a_1} - 1 \right) \frac{X}{2\eta_l}, \text{ for cyclic loading} \\ 1 + 2 \left( \frac{1}{a_1} - 1 \right) \frac{X}{\eta_l}, \text{ for monotonic loading} \end{array} \right\} \geq 1 \quad (2)$$

where  $G_{\max}$  is the maximum (small-strain) shear modulus and  $T$  is a dimensionless scalar that varies during loading introducing  $G_t$  degradation (and as an effect hysteretic damping  $\xi$ ). In particular, the  $G_{\max}$  of Eq. (1) is either quantified as a function of the (small strain) shear wave velocity  $V$  of the soil (and its mass density  $\rho$ ), via  $G_{\max}=\rho V^2$ , or estimated as a function of the mean effective pressure  $p$  and the void ratio  $e$  of the soil, via:

$$G_t = \frac{G_{\max}}{T} = \left( \frac{B p_a}{0.3 + 0.7 e^2} \sqrt{\frac{p}{p_a}} \right) \left( \frac{1}{T} \right) \quad (3)$$

where  $B$  is a model constant and  $p_a$  is the atmospheric pressure (e.g.  $p_a=98.1\text{kPa}$ ). In turn, scalar  $T$  of Eq. (2) is a function of “distance”  $X$  in generalized stress-ratio space of the ever-current deviatoric stress ratio tensor  $\mathbf{r}$  ( $= \mathbf{s}/p$ , where  $\mathbf{s}$  is the deviatoric stress tensor and  $p$  is the mean effective stress) from its value  $\mathbf{r}^{\text{ref}}$  at the last reference state, estimated by:

$$X = \sqrt{1/2(\mathbf{r} - \mathbf{r}^{\text{ref}}) : (\mathbf{r} - \mathbf{r}^{\text{ref}})} \quad (4)$$

where  $:$  denotes the double inner product of the 2 tensors. The reference state for monotonic loading is the equilibrium state, while for cyclic loading the reference state is updated at each shear reversal state. In addition, scalar  $\eta_l$  in the denominator of “distance”  $X$  in Eq. (2) provides correlation to the (updating) reference state via:

$$\eta_l = \alpha_1 \left( \frac{G_{\max}^{\text{ref}}}{p^{\text{ref}}} \right) \gamma_1 \quad (5)$$

where  $p^{\text{ref}}$  and  $G_{\max}^{\text{ref}}$  correspond to the values of  $p$  and  $G_{\max}$  (using Eq. (1) for  $T=1$ ) at the last reference state (where also the  $\mathbf{r}^{\text{ref}}$  is updated), while  $\gamma_1$  and  $\alpha_1$  are model constants.

For reasons of simplicity, shear reversal is assumed to be triggered when the  $X$  value reduces from its previous step. Then,  $p^{\text{ref}}$ ,  $G_{\text{max}}^{\text{ref}}$  and  $\mathbf{r}^{\text{ref}}$  are updated rendering “*distance*”  $X$  to be zero, as is its initial value (at the equilibrium state). Given Eq. (2), this updating of the reference state translates to  $G_t = G_{\text{max}}$  (since  $T=1$ , upon unloading), thus ensuring that the response is much stiffer upon each shear reversal than the preceding shear increment. As shearing continues without change in direction (i.e without triggering shear reversal), “*distance*”  $X$  increases, leading  $G_t$  to decrease smoothly, as per Eqs. (1) and (2). Based on the above, the predicted soil response is non-linear hysteretic, leading to practically closed loops when shear cycles are symmetric. This response, and thus this constitutive model, is considered realistic for dry soils or for saturated soils when earthquake-induced excess pore pressures are not significant (e.g. clays, plastic silts and silty sands, or coarse gravels).

The non-linear model has 4 constants, the elastic Poisson’s ratio  $\nu$  (with 0.33 being a commonly assumed value), constant  $B$  (or velocity  $V$ ) that scales the  $G_{\text{max}}$  value, positive scalar  $\alpha_1$  ( $\leq 1$ ) that introduces non-linearity ( $\alpha_1=1$  for  $T=1$  and linear response), and  $\gamma_1$  is a reference cyclic shear strain level. Figure 2 shows example of simulation runs for calibrating constants  $\alpha_1$  and  $\gamma_1$  to best fit the experimental curves of secant shear modulus  $G/G_{\text{max}}$  degradation and hysteretic damping  $\xi$  increase curves with cyclic strain amplitude  $\gamma$  of Vucetic and Dobry (1991). For the purpose of this paper, the small strain shear wave velocities  $V$  (related to  $G_{\text{max}}$  and model constant  $B$  values) for the dam shells and the clay core were considered functions of the initial mean effective stress  $p_o$ , as this was estimated by a staged construction analysis of each studied earth dam (see Andrianopoulos et al. 2012 for details). Constants  $\alpha_1$  and  $\gamma_1$  were chosen on the basis of the calibration of Figure 2, depending on the plasticity index  $PI(\%)$ : 0 – 7.5% for the shells, modeled as a  $PI=0\%$  material, 7.5 – 15% for the clay core, modeled as a  $PI=15\%$  material.

### 3. ESTIMATION OF PEAK SEISMIC COEFFICIENT $k_{hmax}$

The hereby proposed methodology for  $k_{hmax}$  estimation is based on statistical analysis of input data and results of the “*decoupled*” numerical analyses described in Section 2. The basic principles of the methodology are similar to that proposed by Papadimitriou et al. (2010), but the selection of the important problem parameters and the quantification of their effects was guided by the findings of Andrianopoulos et al. (2012). It should be underlined that in comparison to the methodology of Papadimitriou et al. (2010), the hereby proposed methodology has a quite wider range of applicability (due to the wider range of variation of problem parameters in the 110 analyses used here, that are different from the 28 analyses compiled by Papadimitriou et al. 2010), and takes into account in a systematic manner parameters like the stiffness of the foundation soil (introduced via the shear wave velocity  $V_b$  in the respective layer), the exact geometric characteristics ( $z$ ,  $t$ ,  $w$  in Fig. 1) and the location (upstream or downstream) of the failure surface.

In particular, the peak seismic coefficient  $k_{hmax}$  may be estimated in four (4) successive steps, which are presented in detail in the four (4) sub-sections that follow. This step-by-step presentation hopefully assists the applicability in practice, but also enables the explanation of the physical mechanisms which control the value of  $k_{hmax}$ .

#### 3.1 Estimation of PGA and predominant period $T_e$ of the seismic excitation (Step 1)

The seismic hazard study for an earth dam proposes values for the peak ground acceleration ( $PGA_{rock}$ ) and the elastic response spectrum (for 5% damping) at the outcropping bedrock for the various design earthquakes (Maximum Design Earthquake, Operating Basis Earthquake, Reservoir-Induced Earthquake), based on local seismicity and attenuation relations. For any of the design earthquakes, the predominant period  $T_e$  may be estimated as the structural period (or the range of structural periods) leading to the peak spectral accelerations. The

estimation of PGA is based on  $PGA_{rock}$ , but should take into account the potential local amplification due to the foundation soil. Therefore, one may outline two cases:

- (a) the earth dam is founded on rock, and therefore  $PGA = PGA_{rock}$ ,
- (b) the earth dam is founded on a soil layer, of thickness  $H_b$  and average shear wave velocity  $V_b$ , overlying rock (e.g. as shown in Fig. 1).

In the second case, the estimation of PGA should neither be performed via attenuation relations, nor by applying EC8 (or any other code) provisions for soil effects on design spectra. The reason for this suggestion is that such methods are too crude for accurate estimation of soil effects, especially for expensive projects like dams and tall embankments. It is best to use more accurate methods (that take into account the exact soil and excitation characteristics at the site), which can easily be applied nowadays. Hence, this estimation may be performed either via a numerical analysis (e.g. the equivalent-linear method employing SHAKE91, Idriss & Sun 1992) or using an approximate methodology, as for example the multi-variable relations of Bouckovalas & Papadimitriou (2003) that effectively duplicate the results of SHAKE91-type analyses, or even a simplified version thereof, that reads:

$$PGA = PGA_{rock} \frac{1 + 0.85 \left( \frac{PGA_{rock}}{g} \right)^{-0.17} \left( \frac{T}{T_e} \right)^2}{\sqrt{\left( 1 - \left( \frac{T}{T_e} \right)^2 \right)^2 + 1.78 \left( \frac{T}{T_e} \right)^2}} \quad (6)$$

where  $T$  is the non-linear fundamental vibration period of the foundation soil layer (assumed horizontally infinite, without the dam on top) that is estimated as:

$$T = \left( \frac{4H_b}{V_b} \right) \sqrt{1 + 5330 [V_b \text{ (m/s)}]^{-1.3} \left( \frac{PGA_{rock}}{g} \right)^{1.04}} \quad (7)$$

where the term in parentheses in front of the square root depicts the elastic fundamental vibration period of the foundation soil layer.

### 3.2 Estimation of the non-linear fundamental period $T_0$ of the dam vibration (Step 2)

The fundamental period  $T_0$  of dam vibration may be attained as the structural period which yields the peak spectral amplification from the base of the dam up to its crest, i.e. the period where the peak of the pertinent transfer function (in terms of elastic response spectra) is observed. The elastic value  $T_{oe}$  may be obtained by employing results from analyses with very low PGA values (to ensure elastic response of all geomaterials), while the non-linear value  $T_0$  requires employing results from analyses at the desired PGA level.

In terms of the proposed methodology, in order to estimate the non-linear fundamental period  $T_0$  of dam vibration, one needs first to estimate its elastic value,  $T_{oe}$ . A statistical analysis of such values from the numerical analyses leads to:

$$T_{oe} \text{ (s)} = 0.024 H(\text{m})^{0.75} \quad (8)$$

The accuracy of Eq. (8) is evident from Fig. 3, which illustrates the effect of the height  $H$  on the value of the elastic fundamental (eigen)period  $T_{oe}$  of dam vibration. From an analytical point of view, one may also estimate  $T_{oe}$  from a simplification of the proposals of Dakoulas & Gazetas (1985) that may read as:

$$T_{oe} = 2.6 \frac{H}{V_s} \quad (9)$$

where  $V_s$  is the average (elastic) shear wave velocity within the body of the dam. Given that the  $V_s$  value is not known *a priori*, one may solve Eq. (9) for  $V_s$ , given Eq. (8) for  $T_{oe}$ , a procedure that leads to:

$$V_s \text{ (m/s)} = 108.3H(\text{m})^{0.25} \quad (10)$$

In other words, the results of the parametric analyses show that the average (elastic)  $V_s$  ranges from 230 to 360m/s for a dam with a clayey core, with the value increasing as the height of the dam increases due to higher overburden stresses.

In the sequel, the value of the non-linear fundamental period  $T_o$  of the dam vibration is estimated on the basis of its elastic value  $T_{oe}$ , by:

$$\frac{T_o}{T_{oe}} = \begin{cases} 1 + 1.76 \left( \frac{V_b \text{ (m/s)}}{1000} \right)^{0.25} \left( \frac{\text{PGA}}{\text{g}} \right)^{0.75} \left( \frac{T_{oe}}{T_e} \right)^{-0.80} & , T_{oe} > T_e \\ 1 + 1.76 \left( \frac{V_b \text{ (m/s)}}{1000} \right)^{0.25} \left( \frac{\text{PGA}}{\text{g}} \right)^{0.75} & , T_{oe} \leq T_e \end{cases} \quad (11)$$

The increasing effects of PGA and  $V_b$  in Eq. (11) depict the increase of the fundamental period of dam vibration (from  $T_{oe}$  to  $T_o$ ) due to increased non-linearity of the response, originating from enhanced hysteretic damping of the geomaterials (resulting from increasing PGA), but also due to the reduction of the radiation damping at the base of the dam (resulting from an increase of  $V_b$  towards high values of rock formations). The introduction of  $T_e$  in Eq. (11) illustrates that for high frequency (and out-of-phase) seismic excitations, the non-linearity predicted by the second relation in Eq. (11), for  $T_{oe} \leq T_e$ , is too severe and its effect should therefore be reduced, thus leading to the proposal of the first relation in Eq. (11), for  $T_e < T_{oe}$ .

Typical numerical results for the effects of excitation characteristics PGA and  $T_e$  on the value of the dam fundamental period increase ratio  $T_o/T_{oe}$  are presented in Fig. 4. In particular, this figure shows the increasing effect of PGA on the fundamental period increase ratio  $T_o/T_{oe}$  for selected analyses pertaining to  $H = 40$  and  $80\text{m}$ , that are denoted with different symbols (the solid lines simply connect related symbols to highlight the trends). This figure also shows that the effect of PGA becomes less intense, as the ratio  $T_{oe}/T_e$  increases, thus introducing the need for the first relation of Eq. (11).



The overall accuracy of Eq. (11) is evaluated in Fig. 5 against all the numerical results in the database. In particular, each symbol in this figure corresponds to a different analysis and is obtained using as coordinates, on one hand, the value of the dam fundamental period increase ratio  $T_o/T_{oe}$  from the analysis, and, on the other hand, the respective simulated value using Eq. (11). A perfect prediction would locate the symbol on the diagonal of the figure (solid line). The two dashed lines denote the standard deviation of the relative error in the estimation of  $T_o/T_{oe}$ , which in this case is equal to  $\pm 16\%$ , depicting quite satisfactory accuracy.

Finally note that based on Eqs (8) and (11), the methodology implies that reservoir impoundment and the existence or not of stabilizing berms do not appear to affect the fundamental period of dam vibration. The former because hydrodynamic pressures are not important for mildly steeped slopes, while the latter because typical berms are not wide and tall enough to effectively stiffen the overall dynamic response of the dam (Bouckovalas et al 2009, Andrianopoulos et al 2012).

### **3.3 Estimation of the peak acceleration at the dam crest, $PGA_{crest}$ (Step 3)**

By definition, the ratio of  $PGA_{crest}/PGA$  depicts the seismic amplification ratio, in peak value terms, within the dam body, as compared to the outcropping foundation soil. In order to consistently quantify this ratio and to effectively disregard local variations of seismic motion at the very top of dams that are of little practical importance, the value of  $PGA_{crest}$  in this paper is estimated as the maximum value of the resultant acceleration time history in the upper 10% of the dam height. This consistently defined amplification ratio may be considered similar in nature to amplification ratios related to 1D soil effects. As such, its value is expected to be influenced by the non-linear fundamental period of dam vibration  $T_o$ , the predominant period of the excitation  $T_e$  and parameters related to the hysteretic damping of

the dam geomaterials and the radiation damping enabled by the stiffness of the foundation layer at the base of the dam. Based on Papadimitriou et al. (2010), the correlation of the  $PGA_{crest}/PGA$  ratio to the (tuning) period ratio  $T_o/T_e$ , besides being consistent to 1D seismic amplification ratios, also reduces the scatter of pertinent numerical results, as compared to simpler correlations to  $T_o$  or height  $H$  alone. This correlation is corroborated by the numerical data used in this effort, and therefore, the dam amplification ratio  $PGA_{crest}/PGA$  is estimated by:

$$\frac{PGA_{crest}}{PGA} = \begin{cases} \Pi \left( \frac{2T_o}{T_e} \right) & , \quad \frac{T_o}{T_e} \leq 0.5 \\ \Pi & , \quad 0.5 \leq \frac{T_o}{T_e} \leq 1.5 \\ \Pi \left( \frac{2T_o}{3T_e} \right)^{-0.7} & , \quad 1.5 \leq \frac{T_o}{T_e} \end{cases} \quad (12a)$$

with:

$$\Pi = 2.7 \left( \frac{V_b \text{ (m/s)}}{1000} \right)^{0.52} \quad (12b)$$

Based on Eq. (12a), the dam amplification ratio  $PGA_{crest}/PGA$  is estimated by a design spectrum type relation, which has a fixed maximum value of  $\Pi$ , Eq. (12b), for a range of predominant excitation periods  $T_e$  close to the non-linear fundamental period  $T_o$  of dam vibration, while it reduces with an increase of the (tuning) period ratio  $T_o/T_e$ , in a manner reminiscent of acceleration design spectra in code provisions for buildings due to out-of-phase vibration. Obviously, for very short dams (very small  $T_o/T_e$  values) the seismic amplification also reduces, since the whole dam vibrates practically similarly to its base.

Furthermore, in principle, the value of  $\Pi$ , should be related to the two damping components, of hysteretic (via  $PGA$ ) and radiation (via  $V_b$ ) type, just like it was performed in Step 2, Eq. (11), for the fundamental period increase ratio  $T_o/T_{oe}$ . Nevertheless, the analysis of the data

did not yield any statistically important effect of PGA on the value of  $PGA_{crest}/PGA$  in general, or particularly on the value of  $\Pi$ . This is probably due to the fact that this effect is already incorporated, to a large degree, via the use of  $T_o$  instead of  $T_{oe}$  in Eq. (12), a parameter that is strongly influenced by PGA (see exponent 0.75 in Eq. 11). On the contrary, the same statistical analysis yielded a strong correlation of the value of  $\Pi$  to the shear wave velocity  $V_b$  via Eq. (12b) that depicts the reduced seismic amplification within the dam body if this is founded on a soft layer, as opposed to firm soil or rock conditions, due to an increase of the related radiation damping. The need for this strong correlation is also implied by the fact that the effect of radiation damping, via  $V_b$ , was not found equally important for the estimation of  $T_o$ , since the pertinent exponent was just 0.25 in Eq. (11).

As an example, Fig. 6 presents a comparison of selected data (symbols) from the numerical database, for the extreme cases of dams over foundation layers having  $V_b = 250\text{m/s}$  and  $1500\text{m/s}$ , to the pertinent (solid line) predictions using Eq. (12). The data show that this effect of radiation damping is very important indeed for the dam response (a factor of more than 2.5 near resonance), and also that for out-of-phase excitations ( $T_o > T_e$ ) the seismic amplification within the dam body is reduced considerably in comparison to its maximum value for excitations with predominant periods  $T_e$  near the non-linear fundamental period  $T_o$  of the dam. Moreover, Fig. 6 shows that Eq. (12) predicts both effects quite satisfactorily. It should be underlined that Papadimitriou et al. (2010) did not have enough data to establish a relation between  $PGA_{crest}/PGA$  and  $V_b$  and had simply proposed two relations, one for (really) soft conditions with  $V_b = 250\text{m/s}$  and the other for firm ground or rock foundation with much higher  $V_b$  values.

The overall accuracy of Eq. (12) is depicted in Fig. 7 against all the numerical results in the database (in the format of Fig. 5). A satisfactory agreement is observed here with a standard deviation of the relative error equal to  $\pm 27\%$ .

Finally note that based on Eq. (12), the methodology implies that reservoir impoundment and the existence or not of typical stabilizing berms do not appear to affect the  $PGA_{crest}$  values. This is attributed to the same reasons that these parameters do not affect the fundamental period of dam vibration  $T_o$  (see Section 3.2, and Andrianopoulos et al 2012 for details).

### **3.4 Estimation of peak seismic coefficient $k_{hmax}$ as a function of $PGA_{crest}$ (Step 4)**

According to Makdisi and Seed (1978), the value of the peak seismic coefficient  $k_{hmax}$  may be satisfactorily normalized over the peak acceleration at the dam crest  $PGA_{crest}$ , a parameter that, based on Section 3.3), reflects the effects of excitation characteristics ( $PGA$ ,  $T_e$ ), dam geometry ( $T_o$ ) and foundation conditions ( $V_b$ ). Moreover, it is well established that for a fixed dam-foundation-excitation combination, and therefore a fixed  $PGA_{crest}$  value, the  $k_{hmax}$  values reduce as the maximum depth  $z$  (from the dam crest, see Fig. 1) of the failure surface increases (Makdisi and Seed 1978, Papadimitriou et al. 2010). This because accelerations generally decrease within the dam body as compared to the dam crest, but also because the large sliding mass of a deep seated failure surface includes points that vibrate out-of-phase, thus reducing the maximum value of the resultant acceleration of the sliding mass, that is quantified via  $k_{hmax}$ . Yet, Andrianopoulos et al. (2012) showed that the design curve of Makdisi and Seed (1978) for estimating the  $k_{hmax}/(PGA_{crest}/g)$  ratio as a reducing function of the normalized maximum depth ratio  $z/H$  is qualitatively accurate, but is accompanied by significant scatter and a clear bias of their proposal towards intermediate height  $H$  dams (40 – 80m).

To explore this effect of dam height  $H$  on the  $k_{hmax}/(PGA_{crest}/g)$  ratio, Fig. 8 focuses on a subset of the numerical database, that corresponds to  $k_{hmax}/(PGA_{crest}/g)$  values for various sliding masses pertaining to dams with height  $H = 20, 40$  and  $80m$  (denoted by different symbols), founded on a stiff soil or soft rock layer (e.g. marl) with  $V_b = 500m/s$  and being

excited with mild intensity motions of  $PGA = 0.15g$  having exceptionally different predominant periods, namely  $T_e = 0.49\text{sec}$  (solid symbols) and  $T_e = 0.15\text{sec}$  (hollow symbols). Specifically, in Figure 8b, the  $k_{h\max}/(PGA_{\text{crest}}/g)$  values are correlated to the normalized maximum depth ratio  $z/H$ , i.e. as proposed by Makdisi and Seed (1978). Careful examination reveals that the effect of dam height  $H$  persists, while the solid symbols always plot to the right of their respective hollow counterparts, clearly denoting that low frequency motions ( $T_e = 0.49\text{sec}$ ) lead to higher  $k_{h\max}/(PGA_{\text{crest}}/g)$  values for the same failure surface, as compared to high frequency motions ( $T_e = 0.15\text{sec}$ ). These consistent effects underline the need for a new correlation.

Hence, in order to alleviate the bias in terms of dam height  $H$ , Fig. 8a simplifies the correlation by introducing depth  $z$  as the design parameter, in a manner reminiscent of the stress reduction factor  $r_d$  in the liquefaction potential methodology of Youd and Idriss (2001). Observe that the reducing effect of  $z$  is verified by the data, but the overall scatter is not reduced. In addition, the consistent bias in terms of  $T_e$  on the  $k_{h\max}/(PGA_{\text{crest}}/g)$  values remains. Alternatively, Figure 8c explores the use of the predominant shear wavelength in the dam body, denoted as  $\lambda_d$ , as the normalizing parameter of maximum depth  $z$ . In concept, this type of normalization takes into account the fact that relatively large predominant shear wavelengths  $\lambda_d$  lead to in-phase vibration of different locations within a sliding mass (of maximum depth  $z$ ) and therefore larger values of  $k_{h\max}/(PGA_{\text{crest}}/g)$ , as compared to the  $k_{h\max}/(PGA_{\text{crest}}/g)$  values pertaining to relatively small  $\lambda_d$  values but the same  $z$ . This trend is indeed verified in Fig. 8c that shows a decreasing effect of the normalized maximum depth ratio  $z/\lambda_d$  on the value of the  $k_h/(a_{\max,\text{crest}}/g)$  ratio, with relatively small scatter and no consistent bias (neither in terms of  $H$ , nor in terms of  $T_e$ ).

It should be noted that  $\lambda_d$  is not known *a priori*, since it is a function of the nonlinear shear wave velocity  $V_{sd}$  and the predominant period of vibration  $T_d$  within the dam body. The

former may be related to  $T_o$  by using Eq. (9) for nonlinear properties ( $T_o$  and  $V_{sd}$  instead of  $T_{oe}$  and  $V_s$ ). On the contrary, the predominant period of vibration  $T_d$  is a new parameter that is equal neither to the predominant excitation period  $T_e$ , nor to the nonlinear fundamental period  $T_o$  of dam vibration. In practice,  $T_d$  usually takes values in between  $T_e$  and  $T_o$  and therefore it is assumed to be approximately equal to their average value. Following this train of thought,  $\lambda_d$  may be approximated as follows:

$$\lambda_d = V_{sd} T_d = \frac{2.6H}{T_o} \left( \frac{T_o + T_e}{2} \right) = 1.3H \left( 1 + \frac{T_e}{T_o} \right) \quad (13)$$

This relation for  $\lambda_d$  was used in the correlation of Fig. 8c, and was also used in the pertinent statistical regression of the whole database. In particular, this regression corroborated the generally decreasing effect of the maximum depth ratio  $z/\lambda_d$ , but also depicted a number of other significant effects. In particular, based on the proposed methodology, the  $k_{hmax}$  may be estimated on the basis of  $PGA_{crest}$  (from Step 3) and  $z/\lambda_d$  according to:

$$\left( \frac{k_{hmax}}{PGA_{crest}/g} \right) = C_1 - 1.18C_b C_f C_g \left( \frac{z}{\lambda_d} \right) \quad (14a)$$

with:

$$1.0 - 0.65C_b C_f C_g \leq \left( \frac{k_{hmax}}{PGA_{crest}/g} \right) \leq 1.0 \quad (14b)$$

where the various C coefficients included in Eq. (14) are related to the (upstream or downstream) location of the sliding mass ( $C_i$ ), large stabilizing berms ( $C_b$ ), the stiffness of foundation layer ( $C_f$ ) and geometric characteristics of the sliding mass ( $C_g$ ) other than maximum depth  $z$ , as explained in the sequel.

Figure 9 illustrates the so-called “*fundamental*” relation of  $k_{hmax}/(PGA_{crest}/g)$  reduction with the normalized maximum depth ratio  $z/\lambda_d$  of the sliding mass that is based on, the also

presented, pertinent numerical data. The term “*fundamental*” relation used here denotes that all C coefficients of Eq. (14) are taken equal to 1.0, thus leading to presentation of only the pertinent numerical data in Fig. 9, i.e. the data that correspond to cases where the dam is founded on stiff soil or any type of rock ( $V_b \geq 500\text{m/s}$ ) and does not have typical stabilizing berms, or if it does have such berms the sliding masses are shallow and do not include them (practically leading to  $z < 0.67H$  for the performed analyses). In addition, the presented data correspond to “*bulky*” (and not “*thin*”) sliding masses (see definitions below), which are not in contact to the reservoir water (if this exists), i.e. for analyses that correspond to earthquake loading at the end of construction, and for downstream sliding masses in the case of a full reservoir (steady state seepage conditions). Observe the relatively small scatter of the data and the fact that the reducing effect of  $z/\lambda_d$  saturates at  $k_{h\max}/(\text{PGA}_{\text{crest}}/g) = 0.35$ , which poses as a lower limit, and requires the introduction of an inequality at the left hand side of Eq. (14b).

From the effects introduced via the C coefficients in Eq. (14), the emphasis is put now on the effect of reservoir impoundment. In particular, Fig 10 presents numerical data in the  $k_{h\max}/(\text{PGA}_{\text{crest}}/g)$  versus  $z/\lambda_d$  format, for upstream sliding masses, that would otherwise be considered as corresponding to the “*fundamental*” relation, namely  $C_b = C_f = C_g = 1.0$ . Therefore, Fig. 10 also includes the “*fundamental*” relation of Fig. 14 and shows that the upstream data plot above but in parallel to the “*fundamental*” relation. Hence, a best-fit average relation for these data can be established by a mere translation of the decreasing curve to larger values of  $k_{h\max}/(\text{PGA}_{\text{crest}}/g)$ , thus giving birth to coefficient  $C_1$  in Eq. (14a). Moreover, the fact that  $k_{h\max}/(\text{PGA}_{\text{crest}}/g)$  never exceeds 1.0, yielded the need for including the inequality at the right hand side of Eq. (14b), of significance only for upstream sliding masses.

By performing similar data selection and statistical analysis, the following values or relations for the C “*correction*” coefficients were hereby estimated:

- $C_1$  is the *location coefficient*, which takes a value of 1.08 for upstream sliding masses of an impounded dam, and a value of 1.0 in any other case. Note that the relatively higher  $k_{hmax}$  values for upstream sliding masses are attributed to amplification phenomena in the pertinent shell due to the stiffness contrast between the saturated (and hence softer) upstream shell as compared to the non-saturated (and hence stiffer) downstream shell of a zoned earthdam at conditions of steady state seepage.
- $C_b$  is the *berm coefficient*, which takes a value of 0.96 if the sliding mass includes a typical stabilizing berm, and a value of 1.0 in any other case. It should be noted that the slightly higher  $k_{hmax}$  values for sliding masses that include a typical stabilizing berm are attributed to topographic amplification phenomena observed in the vicinity of such berms, similarly to what is observed near any single-faced slope of related dimensions (e.g. Bouckovalas and Papadimitriou 2005). Yet, these effects are practically local and do not affect consistently the overall dam response (e.g. values of  $T_o$  and  $PGA_{crest}$  remain essentially unaffected, see Bouckovalas et al. 2009, Andrianopoulos et al 2012)
- $C_f$  is the *foundation coefficient*, which is given by:

$$C_f = \begin{cases} 0.38 + 1.24 \left( \frac{V_b(m/s)}{1000} \right), & V_b < 500m/s \\ 1.00 & , \quad V_b \geq 500m/s \end{cases} \quad (15)$$

The form of Eq. (15) denotes that there is a small consistent amplifying effect on  $k_{hmax}/(PGA_{crest}/g)$  values for earth dams founded on a soft soil layer (of significant thickness, i.e. more than 5m). Note that low  $V_b$  values (leading to  $C_f < 1$ ) are considered practically possible only for relatively short dams (e.g.  $H \leq 30m$ ). This is due to the fact



that for taller earthdams a relatively soft foundation layer could make the construction of the dam problematic (e.g. excessive settlements).

- $C_g$  is the *geometry coefficient* of the sliding mass, which is given by:

$$C_g = \begin{cases} 0.91, & \text{if } (t/w) \leq 0.14 \quad (\text{i.e. for "thin" sliding mass}) \\ 1.00, & \text{if } (t/w) > 0.14 \quad (\text{i.e. for "bulky" sliding mass}) \end{cases} \quad (16)$$

with the  $w$  and  $t$  being geometrical characteristics of the sliding mass, corresponding to its width (in the horizontal direction) and the maximum distance between two lines that are parallel to the points of entry and exit of the failure surface and adjoin the sliding mass (see Fig. 1, for illustrated definition). Obviously, small  $(t/w)$  ratios correspond to relatively elongated thin sliding masses, thus the use of the term “*thin*” in Eq. (16), while for large  $(t/w)$  ratios the sliding masses are relatively bulky, thus the homonymous term in Eq. (16). The relatively higher values of  $k_{hmax}$  for “*thin*” as opposed to “*bulky*” sliding masses with the same maximum depth  $z$  are attributed to the fact that the former include mostly surficial locations of the dam body where higher accelerations are expected as compared to the heavier latter sliding masses.

Figure 11 evaluates the overall accuracy in the prediction of the peak seismic coefficient  $k_{hmax}$  for all 1084 sliding masses in the numerical database. A satisfactory accuracy is depicted with a standard deviation of the relative error equal to  $\pm 27\%$  (see dashed lines). In order to fully ascertain the appropriateness of the proposed methodology, Fig. 12 studies the relative error in the prediction of  $k_{hmax}$ , denoted as  $R_{k_{hmax}}$ , which is defined as the ratio of the difference of the predicted value of  $k_{hmax}$  minus the  $k_{hmax}$  from the analyses over the latter value. Hence, positive values of  $R_{k_{hmax}}$  correspond to overprediction, while negative to underprediction of the peak seismic coefficient. In particular, this figure plots the  $R_{k_{hmax}}$  values for all 1084 sliding masses against the (tuning) period ratio  $T_o/T_e$  (in plot a), the normalized maximum depth ratio  $z/\lambda_d$  (in plot b) and the PGA (in plot c), while different

symbols denote different dam heights  $H$ . It is thus observed that there is no consistent bias of overprediction or underprediction for any of the important problem parameters.

#### 4. ESTIMATION OF EFFECTIVE SEISMIC COEFFICIENT $k_{hE}$ ON THE BASIS OF ALLOWABLE DISPLACEMENTS

The previous section described a stand-alone, user-friendly methodology for estimating the peak seismic coefficient  $k_{hmax}$ , given the excitation characteristics ( $PGA_{rock}$ ,  $T_e$ ), the foundation conditions ( $H_b$ ,  $V_b$ ), the characteristics of the dam ( $H$ ,  $V_s$ ) and of the sliding mass ( $z$ ,  $w$ ,  $t$ , location, etc). In this section, a methodology will be proposed for estimating the “effective” seismic coefficient  $k_{hE}$  (for use in pseudo-static analyses) as a percentile of its peak value, on the basis of:

$$k_{hE} = k_{hmax} / q \quad (17)$$

where  $q$  ( $\geq 1$ ) is the *sliding factor* that is to be correlated to allowable downslope deviatoric displacements  $D_{all}$ .

To do so, one may assume that the slope is at a state of limit equilibrium ( $FS_d = 1.0$ ) when the inertial acceleration is equal to  $k_{hE}g$ , i.e.  $k_{hE} = k_y$ . In this way, and given Eq. (17), the slope is allowed to develop downslope deviatoric displacements, since the peak acceleration of the sliding mass  $k_{hmax}g$  corresponds to  $FS_d < 1$ . The amount of these displacements may be estimated using Newmark’s sliding block procedure, given  $k_{hmax}$  and  $k_y$ . Here, the opposite is required, namely to correlate the  $q = k_{hmax}/k_y$  to the given allowable downslope deviatoric displacements  $D_{all}$ . For this purpose one may employ any of the (many) displacement equations for sliding blocks available the literature and solve for  $k_y$ , i.e. the only parameter that is common in all equations. This train of thought was followed by Bray and Travararou (2009), who employed the equation of Bray and Travararou (2007) that was based on

“*coupled*” analyses. In this effort, the analyses performed were “*decoupled*” and therefore, for consistency, the few available displacement equations/charts that are based on “*decoupled*” analyses (Makdisi and Seed 1978, Bray and Rathje 1998) were entertained as initial options. However, none of them was finally opted, since the former uses a non-engineering parameter (earthquake magnitude  $M$ ) in its formulation and was based on relatively few recordings available at that time, while the latter uses the  $PGA_{rock}$  as an intensity measure, which is related to the base excitation but not the actual dam vibration.

Then, the large family of rigid sliding block displacement equations was considered as a pool for selecting an appropriate equation. The basic premise here is that such an equation may be accurately used for a flexible sliding block, if the seismic intensity measures accounted for in the equation are not those of the plane (e.g.  $PGA$ ,  $PGV$ ), but of the sliding block itself (e.g.  $a_{hmax}=k_{hmax}g$ , peak velocity of the sliding mass  $v_{hmax}$ , respectively) estimated on the basis of the “*decoupled*” analyses. It is well known that this family of equations employs many different types and combinations of intensity measures:  $PGA$  (common in practically all equations),  $PGV$  (e.g. Newmark 1965, Franklin and Chang 1977, Richards and Elms 1979, Whitman and Liao 1984, Cai and Bathurst 1996, Saygili and Rathje 2008), predominant period  $T_e$  (e.g. Sarma 1975, Ambraseys and Menu 1988, Yegian et al. 1991), Arias intensity  $I_a$  (Jibson 2007), and in some cases the earthquake magnitude  $M$  (e.g. Saygili and Rathje 2008) or even the number of significant excitation cycles  $N$  (e.g. Yegian et al 1991). Hence, in the selection process, it was considered essential to consider equations including  $PGV$  (in order to take into account the frequency content of the excitation), and to avoid equations that employ parameters that are non-engineering ( $M$ ) and not so well-established in engineering practice ( $I_a$ ,  $N$ ).

Figure 13 compares the range of displacement  $D$  predictions from the parametric study of Franklin and Chang (1977) to a series of equations that meet the foregoing criteria (and are

provided in Table 1), namely:

- several upper-bound (UB) equations: Newmark (1965), Richards and Elms (1979), Cai and Bathurst (1996), and
- one average (AVE) equation: Whitman and Liao (1984).

Note that the employed plotting scheme normalizes displacements  $D$  with parameter  $PGV^2/PGA$  (that also measures in m), while the horizontal axis plots the ratio of  $k_y/(PGA/g)$  and provides generalization for all possible combinations of  $k_y$ ,  $PGA$  and  $PGV$ . Hence, other equations that also meet the previously set criteria (e.g. Saygili and Rathje 2008; see Table 1), but are unable to be plotted and compared in Fig. 13 due to the selected generalization scheme, had to be excluded from the pool of options.

Based on this figure it may be concluded that the equation of Whitman and Liao (1984) is considered appropriate for an average fit of the depicted range of sliding block displacement predictions, while the equation of Cai and Bathurst (1996) is considered appropriate for an upper bound fit. Note that, if one replaces  $PGA$  with  $k_{hmax}g$  and  $PGV$  with  $v_{hmax}$  in any of the equations of Table 1, he may then attempt to solve for  $k_y$  or better directly for the *sliding factor*  $q = k_{hmax}/k_y$ . This can be readily done for the equation of Whitman and Liao (1984), but not for the equation of Cai and Bathurst (1996). Hence, the latter was replaced with the one denoted as “*proposed*” in Figure 13 and Table 1, that fits it with a simpler analytical form. Doing so yields the following equations for upper bound  $q_{UB}$  and average  $q_{AVE}$  estimates of the *sliding factor*:

$$q = \frac{k_{hmax}}{k_{hE}} = \left\{ \begin{array}{l} \frac{-8}{\ln \left( D_{all} / \left[ 90 \frac{v_{hmax}^2}{k_{hmax}g} \right] \right)} \quad (=q_{UB}), \text{ for conservatism} \\ \frac{-9.4}{\ln \left( D_{all} / \left[ 37 \frac{v_{hmax}^2}{k_{hmax}g} \right] \right)} \quad (=q_{AVE}), \text{ for average estimates} \end{array} \right\} \geq 1 \quad (18)$$

The graphical form of  $q_{UB}$  and  $q_{AVE}$  is presented in Fig. 14. Focusing first on  $q_{UB}$  it becomes obvious that  $q_{UB} = 1$  for very small displacements,  $D_{all} < 0.03[v_{hmax}^2/(k_{hmax}g)]$ , and exceeds a value of 2 for quite larger displacements  $D_{all} > 1.65[v_{hmax}^2/(k_{hmax}g)]$ . Furthermore, note that always  $q_{AVE} > q_{UB}$  for the same value of allowable displacements  $D_{all}$ , i.e. the  $k_{hE}$  values are larger when employing  $q_{UB}$  rather than  $q_{AVE}$  for the same  $k_{hmax}$ , thus leading to more conservative design. Careful examination of Eq. (18) shows that the ratio of  $q_{AVE}/q_{UB}$  ranges between 1.3 and 2, and exceeds 2 only for extremely large values of  $D_{all} > 10.44[v_{hmax}^2/(k_{hmax}g)]$ . It should be underlined that although this figure has been drawn for  $q$  values up to 10, it is not advised to use such large values in the design of earthdams due to the crudeness of employing rigid sliding block equations for such large overall downslope displacements.

Note that a similar assumption was recently used by Rathje and Antonakos (2011) who replaced PGA and PGV of the rigid sliding block displacement equation of Saygili and Rathje (2008) with  $k_{hmax}g$  and  $v_{hmax}$  from “*coupled*” analyses in order to estimate flexible sliding mass displacements. In their effort, they show that such an approach is rational, but it may underestimate displacements for very flexible sliding masses. This may be attributed to the fact that their  $k_{hmax}/(PGA/g)$  ratios usually fall significantly below 1.0 for flexible sliding masses (may reach values of 0.1, on average, for very flexible masses). This is not observed in data from “*decoupled*” analyses, which show values for the  $k_{hmax}/(PGA/g)$  ratio that are consistently below 1.0, on average, only for deep sliding masses ( $z/H > 0.7$ ) and especially for out-of-phase dam vibrations ( $T_o/T_e > 2$ ), but even then, this ratio does not reach values

lower than 0.4, on average (e.g. Andrianopoulos et al. 2012). In any case, the use of  $q_{UB}$  rather than  $q_{AVE}$  of Eq. (18), along with a “*decoupled*” estimation of  $k_{hmax}$  in Section 3 may be considered sufficient to alleviate all concerns regarding non-conservatism of the proposed methodology.

The only parameter not quantified in Eq. (18) is the value of  $v_{hmax}$ , i.e. the peak velocity of the sliding mass. This will not be estimated as a separate quantity; but through the ratio of the peak velocity over the peak acceleration of the sliding mass ( $v_{hmax}/a_{hmax}$ ) a quantity that may be related to the vibration period of the sliding mass, similarly to how the PGV/PGA ratio is related to the predominant period  $T_e$  of a seismic recording (e.g.  $T_e = 4.3(PGV/PGA)$  according to Fajfar et al. 1992). By relating this ratio to the predominant period of dam vibration  $T_d = (T_o + T_e)/2$  (see Eq. 13) and the normalized maximum depth of the sliding mass ( $z/\lambda_d$ ), a statistical regression of numerical data yielded the following equation:

$$\frac{v_{hmax}}{a_{hmax}} (\text{sec}) = \frac{v_{hmax}}{k_{hmax}g} (\text{sec}) = 0.071 [1 + 1.48 T_d] \left( \frac{z}{\lambda_d} \right)^{0.12} \quad (19)$$

This relation shows that the ( $v_{hmax}/a_{hmax}$ ) ratio increases practically linearly with an increase in the significant periods  $T_e$  and  $T_o$  of the problem, and that it also increases slightly as the sliding mass becomes deeper, and thus more flexible. Figure 15 presents the overall accuracy in the prediction of the ratio ( $v_{hmax}/a_{hmax}$ ), and thus of the peak velocity of the sliding mass  $v_{hmax}$ , for all 1084 sliding masses in the numerical database. Based on this, a very satisfactory accuracy is depicted with a standard deviation of the relative error equal to  $\pm 19\%$ .

## 5. DISCUSSION

Despite significant research invested to estimating seismic coefficients for the design of earthdams and tall embankments, there is still need for a methodology that establishes a correlation between the well-established pseudo-static analysis of such geostructures and modern performance-based design principles. The hereby proposed methodology is based on statistical analysis of input data and results from “*decoupled*” seismic response analyses and is stand-alone, i.e. it provides end-results without resorting to other methodologies. Furthermore, it is simple, as it may be programmed in a worksheet, and leads to satisfactory accuracy in the estimation of the peak seismic coefficient  $k_{hmax}$  with a standard deviation of the relative error equal to  $\pm 27\%$  in comparison to case-specific non-linear numerical analyses. To allow for the performance-based seismic design of earthdams, a *sliding factor*  $q$  ( $\geq 1$ ) is defined that divides the  $k_{hmax}$  value to yield the “*effective*” seismic coefficient  $k_{hE}$ , which is to be used for pseudo static analyses with a requirement of  $FS_d \geq 1.0$ . The value of the *sliding factor* is estimated on the basis of allowable slope displacements  $D_{all}$ , peak seismic intensity indices for the sliding mass (peak acceleration  $a_{hmax}$  and velocity  $v_{hmax}$ ) and the desired level of conservatism (upper-bound or average).

The basic premise of the proposed methodology for estimating  $k_{hmax}$  is the use of “*decoupled*”, and not “*coupled*” analyses for its purpose. This choice may come as a surprise, given that the latter analyses are currently the state-of-the-art for slope stability issues, with many benefits arising from their use (e.g. less computational effort). Nevertheless, the former type of analyses comprises the state-of-practice world-wide (e.g. Rathje and Antonakos 2011), especially for earthdams. Moreover, only such analyses give emphasis to aspects of dam vibration (e.g. effects of dam resonance (for  $T_o/T_e \cong 1$ ) and soil foundation stiffness) that have been proven to be significant for the values of  $k_{hmax}$  (e.g. Zania et al 2011, Papadimitriou et al. 2010, Andrianopoulos et al. 2012). In addition, it was desired to

investigate whether typical stabilizing berms and reservoir impoundment affect the values of the seismic coefficients of earthdams, as well to ascertain the relative importance of the exact geometry of the sliding mass (besides its maximum depth  $z$ ), all issues that could only be addressed by “*decoupled*” analyses. The foregoing benefits of using “*decoupled*” analyses come at a price of conservatism for sliding masses of shallow and intermediate depth, but also a tendency for non-conservatism for flexible (deep) sliding masses, and this especially for high ratios of  $k_y/k_{hmax}$  (e.g. Kramer and Smith 1997, Rathje and Bray 2000). Focusing on the latter problem (which is of main concern for practitioners), it is important to note that this non-conservatism is generally related to small displacements, due to the high values of  $k_y/k_{hmax}$  mentioned above, in combination with small values of  $k_{hmax}$  observed for flexible masses (Rathje and Antonakos 2011). Hence, the use of a “*decoupled*” approach may be considered “*reasonably accurate*” for flexible sliding masses, an assertion independently confirmed by experimental work (Wartman et al. 2003). In any case, as far as the proposed methodology is concerned, the end-user may partly adjust the desired level of conservatism when selecting the *sliding factor*  $q$ , i.e. values of  $q_{UB}$  or  $q_{AVE}$  or anything in between, although the use of  $q_{UB}$  is recommended by the authors, at least for preliminary design stages. Overall, the methodology is considered reliable for use in the design of:

- (a) Earthdams or tall embankments, with height  $H$  ranging from 20 to 120m, of triangular or trapezoidal cross section, with or without typical stabilizing berms (e.g. of height and width up to  $H/3$  and  $2H/3$ ), for end of construction and steady state seepage conditions, that are founded on ground with shear wave velocities  $V_b$  higher than 250m/s (firm soil or rock),
- (b) Seismic excitations with predominant periods  $T_e = 0.14$  to 0.50s and peak accelerations PGA at the free-field of the foundation soil reaching up to 0.50g.



Of interest is also the fact that the methodology is applied in independent steps of generic value, given the parametric nature of the performed analyses. Specifically, if one has independently estimated the PGA (Step 1, section 3.1) or even the non-linear fundamental period  $T_0$  of a geostructure (Step 2, section 3.2), he may apply only the remaining Steps 3 and 4 for estimating the peak seismic coefficient  $k_{hmax}$ , without loss of accuracy. Also, specific steps of the methodology may be used in aid of other existing methodologies (e.g. Step 3 for estimating the  $PGA_{crest}$  may be used in combination with the Makdisi and Seed 1978 procedure, which does not explicitly provide an equation or design chart for its estimation).

Given that the methodology was based on plane strain analyses, the earthdam or tall embankment in question should be sufficiently long as to allow for an accurate 2D approximation. Moreover, ground movements (e.g. crest settlements) due to volumetric densification are not captured by Newmark-type models. Hence, the  $D_{all}$  to be used in this methodology to estimate the *sliding factor*  $q$  should refer only to deviatoric-induced displacements, while densification-induced displacements should be accounted for separately, on the basis of relevant methodologies (e.g. Tokimatsu and Seed 1987). Furthermore, the methodology emphasizes on seismic coefficients related to the horizontal sliding mass vibration, and there is no reference made to the vertical component of motion. This is consistent with all pertinent methodologies in the literature, both “*coupled*” and “*decoupled*”, but is also backed by recent evidence (Christchurch earthquake) showing that for sliding systems even large vertical acceleration components have only a negligible effect (Gazetas et al 2012). Finally, it should be underlined that the performed analyses, as well as the proposed methodology, do not take into account shear strength degradation of the geomaterials comprising the earthdam. The literature includes elegant and simple procedures for incorporating such issues in seismic slope stability analyses (e.g. Biondi et al. 2002 incorporate the effects of excess pore pressure buildup in assessing the stability of infinite

cohesionless slopes). Yet, given the complexity of such issues and the importance of infrastructure works like earthdams or tall embankments, the authors believe that robust numerical analyses with advanced constitutive models (e.g. NTUA-SAND of Andrianopoulos et al. 2010 for liquefiable soils) should remain the seismic analysis tool for such geotechnical structures.

## **6. ACKNOWLEDGEMENTS**

The authors would like to thank the Public Power Corporation of Greece S.A. for funding this research, as well as Civil Engineers Angelos Zographos, Sofia Tsakali and Stavroula Stavrou for performing the numerical analyses on which the proposed methodology was based.

## **7. REFERENCES**

1. Ambraseys N. N., Menu J. M. (1988), "Earthquake-induced ground displacements", *Earthquake Engineering and Structural Dynamics*, Vol. 16, pp. 985–1006
2. Andrianopoulos K. I. (2006), "Numerical modeling of static and dynamic behavior of elastoplastic soils, Doctorate Thesis, Department of Geotechnical Engineering, School of Civil Engineering, National Technical University of Athens (in Greek)
3. Andrianopoulos K. I., Papadimitriou A. G., Bouckovalas G. D. (2010), "Bounding surface plasticity model for the seismic liquefaction analysis of geotechnical structures", *Soil Dynamics and Earthquake Engineering*, Vol. 30, No. 10, pp. 895-911
4. Andrianopoulos K. I., Papadimitriou A. G., Bouckovalas G. D., Karamitros D. K. (2012), "Insight to seismic response of earthdams, with emphasis on seismic coefficient estimation", *Computers and Geotechnics* (under review)
5. Biondi G., Cascone E., Maugeri M. (2002), "Flow and deformation failure of sandy slopes", *Soil Dynamics and Earthquake Engineering*, 22(9-12): 1103-1114
6. Biondi G., Cascone E., Rampello S. (2007), "Performance-based pseudo-static analysis of slopes", 4<sup>th</sup> International Conference on Earthquake Geotechnical Engineering, Thessaloniki, Greece, June 25-28
7. Bouckovalas G. D., Papadimitriou A. G. (2003), "Multi-variable relations for soil effects on seismic ground motion", *Earthquake Engineering and Structural Dynamics*, 32: 1867-1896, Wiley

8. Bouckovalas G. D., Papadimitriou A. G. (2005), "Numerical Evaluation of Slope Topography Effects on Seismic Ground Motion", *Soil Dynamics and Earthquake Engineering*, 25(7-10): 547 - 555
9. Bouckovalas G. D., Papadimitriou A. G., Andrianopoulos K. I. (2009), "Estimation of seismic coefficients for the slope stability of earthdams: Phase B", Research Report to Public Power Corporation, p. 269 (in Greek)
10. Bozbey I., Gundogdu O. (2011), "A methodology to select seismic coefficients based on upper bound "Newmark" displacements using earthquake records from Turkey", *Soil Dynamics and Earthquake Engineering*, 31, 440-451
11. Bray J. D., Rathje E. M. (1998), "Earthquake-induced displacements of solid-waste landfills", *Journal of Geotechnical and Geoenvironmental Engineering*, ASCE 124 (3), 242-253
12. Bray J. D., Travasarou T. (2007), "Simplified procedure for estimating earthquake – induced deviatoric slope displacements", *Journal of Geotechnical and Geoenvironmental Engineering*, ASCE, 133(4):381-392
13. Bray J. D., Travasarou T. (2009), "Pseudostatic coefficient for use in simplified slope stability evaluation", *Journal of Geotechnical and Geoenvironmental Engineering*, ASCE, 135(9):1336-1340
14. Cai Z., Bathurst R. J. (1996), "Deterministic sliding block methods for estimating seismic displacements of earth structures", *Soil Dynamics and Earthquake Engineering*, 15, 255-268
15. Charles J. A., Abiss C. P., Gosschalk E. M., Hinks J. L. (1991), "An engineering guide to seismic risk to dams in the United Kingdom", Building Research Establishment Report.
16. Dakoulas P., Gazetas G. (1985). "A class of inhomogeneous shear models for seismic response of dams and embankments", *Soil Dynamics and Earthquake Engineering*, 4(4): 166-182
17. Fajfar P, Vidic T, Fischinger M. (1992), "On energy demand and supply in SDOF systems". In *Nonlinear Seismic Analysis of RC Buildings*, Fajfar P, Krawinkler H. (eds). Elsevier: Amsterdam, 41-61.
18. Franklin A. G., Chang F. K. (1977), "Permanent displacement of earth embankments by Newmark sliding block analysis", Misc. Paper S-71-17, Soil and Pavement Labs, US Army Eng. Waterways Expt. Stn., Vicksburg, Miss.
19. Gazetas, G., Garini, E., Berrill, J. B., Apostolou, M. (2012), "Sliding and overturning potential of Christchurch 2011 earthquake records", *Earthquake Engineering and Structural Dynamics*, doi: 10.1002/eqe.2165
20. Hynes-Griffin M. E., Franklin A. G. (1984), "Rationalizing the seismic coefficient method", Miscellaneous Paper GL-84-13, U.S. Army Corps of Engineers Waterways Experiment Station, Vicksburg, Mississippi, 21 pp
21. Idriss I. M., Sun J. I. (1992), "SHAKE91 – A computer program for conducting equivalent linear seismic response analysis of horizontally layered soil deposits. User's Guide", Center for Geotechnical Modeling, Civil Engineering Department, U.C. Davis
22. Itasca Consulting Group Inc (2005), "FLAC – Fast Lagrangian Analysis of Continua", Version 5.0, User's Manual.

23. Jibson R. W. (2007), "Regression models for estimating coseismic landslide displacement", *Engineering Geology*, 91:209–18
24. Kramer S. L., Smith, M. W. (1997), "Modified Newmark model for seismic displacements of compliant slopes" *Journal of Geotechnical and Geoenvironmental Engineering*, 123(7): 635–644
25. Lin J.-S., Whitman, R. V. (1983), "Decoupling approximation to the evaluation of earthquake induced plastic slip in earth dams", *Earthquake Engineering and Structural Dynamics*, 11, 667–678.
26. Makdisi F. H., Seed H. B. (1978), "Simplified procedure for estimating dam and embankment earthquake-induced deformations", *Journal of Geotechnical Engineering Division, ASCE*, 104(7): 849-867
27. Newmark N. (1965), "Effects of earthquakes on dams and embankments", *Geotechnique*, 15(2): 139-160
28. Papadimitriou A. G. (1999), "Elastoplastic modelling of monotonic and dynamic behavior of soils", Doctorate Thesis, Department of Geotechnical Engineering, Faculty of Civil Engineering, National Technical University of Athens, June, (in Greek)
29. Papadimitriou A. G., Andrianopoulos K. I., Bouckovalas G. D., Anastasopoulos K. (2010). "Improved methodology for the estimation of seismic coefficients for the pseudo-static stability analysis of earthdams", *Proceedings, 5th International Conference on Recent Advances in Geotechnical Earthquake Engineering and Soil Dynamics*, May 24-29
30. Ramberg W., Osgood W. R. (1943), "Description of stress-strain curve by three parameters", Technical note 902, National Advisory Committee for Aeronautics
31. Rathje E. M., Antonakos G. (2011). "A unified model for predicting earthquake-induced sliding displacements of rigid and flexible slopes", *Engineering Geology*, Vol. 122, pp. 51-60
32. Rathje E. M., Bray J. D. (2000), "Nonlinear coupled seismic sliding analysis of earth structures", *J. of Geotech. and Geoenviron. Engineering, ASCE*, 126(11):1002-1014
33. Richards R., Elms D. G. (1979), "Seismic behaviour of gravity retaining walls", *Journal of Geotechnical Engineering Division, ASCE*, 105(4), pp. 449-464
34. Sarma S. K. (1975), "Seismic stability of earth dams and embankments", *Geotechnique*, 25(4): 743-761
35. Saygili G., Rathje E. M. (2008), "Empirical predictive models for earthquake-induced sliding displacements of slopes", *Journal of Geotechnical and Geoenvironmental Engineering, ASCE* 134 (6), 790–803
36. Tokimatsu, K., Seed H. B. (1987), "Evaluation of settlements in sands due to earthquake shaking", *Journal of Geotechnical Engineering, ASCE*, 113(8): 861-878
37. USCOLD (1985) "Guidelines for selecting seismic parameters for dam projects", Report of Committee on Earthquakes, U.S. Committee on Large Dams
38. Vucetic M., Dobry R. (1991), "Effect of soil plasticity on cyclic response", *Journal of Geotechnical Engineering, ASCE*, 117(1):89-107
39. Wartman J., Bray J. D., Seed R. B. (2003), "Inclined plane studies of the Newmark sliding block procedure", *Journal of Geotechnical and Geoenvironmental Engineering, ASCE*, 129(8): 673-684

40. Whitman R. V., Liao S. (1984), "Seismic design of gravity retaining walls", Proceedings, 8th World Conference on Earthquake Engineering, San Francisco, 3, pp. 533-540.
41. Youd T. L., Idriss I. M. (2001), "Liquefaction resistance of soils: summary report from the 1996 NCEER and 1998 NCEER/NSF Workshops on Evaluation of Liquefaction Resistance of Soils", Journal of Geotechnical and Geoenvironmental Engineering, ASCE, 127(4): 297 – 313
42. Yegian M. K., Marciano E. A., Ghahraman V. G. (1991), "Earthquake-induced permanent deformations: probabilistic approach", Journal of Geotechnical Engineering, ASCE, 117(1): 1158-1167
43. Zania V., Tsompanakis Y., Psarropoulos P. N. (2011), "Seismic slope stability of embankments: a comparative study on EC8 provisions", Proceedings, ERTC-12 Workshop on Evaluation of Geotechnical Aspects of EC8, Athens, Sept. 11, (ed. M. Maugeri), Patron Editore – Quarto Inferiore – Bologna.

**Table 1:** Form of upper-bound (UB) and average (AVE) prediction equations for rigid sliding block permanent displacements D, as a function of PGA, PGV and  $k_y$

Reference	Equation	UB/AVE <sup>(1)</sup>
Newmark (1965) for $k_y/(PGA/g) < 0.16$	$D=3 \frac{PGV^2}{PGA} \left( \frac{k_y}{PGA/g} \right)^{-1}$	UB
Newmark (1965) for $k_y/(PGA/g) > 0.16$	$D=0.5 \frac{PGV^2}{PGA} \left( \frac{k_y}{PGA/g} \right)^{-2}$	UB
Richards and Elms (1979) for $k_y/(PGA/g) > 0.3$	$D=0.087 \frac{PGV^2}{PGA} \left( \frac{k_y}{PGA/g} \right)^{-4}$	UB
Cai and Bathurst (1996)	$D=35 \frac{PGV^2}{PGA} \exp\left(-6.91 \frac{k_y}{PGA/g}\right) \left( \frac{k_y}{PGA/g} \right)^{-0.38}$	UB
PROPOSED (fit of Cai and Bathurst 1996)	$D=90 \frac{PGV^2}{PGA} \exp\left(-8 \frac{k_y}{PGA/g}\right)$	UB
Whitman and Liao (1984)	$D=37 \frac{PGV^2}{PGA} \exp\left(-9.4 \frac{k_y}{PGA/g}\right)$	AVE
Saygili and Rathje (2008) (D in cm, PGA in g, PGV in cm/s)	$\ln D = -1.56 - 4.58 \left( \frac{k_y g}{PGA} \right) - 20.84 \left( \frac{k_y g}{PGA} \right)^2 + 44.75 \left( \frac{k_y g}{PGA} \right)^3 -$ $-30.5 \left( \frac{k_y g}{PGA} \right)^4 - 0.64 \ln(PGA) + 1.55 \ln(PGV)$	AVE

<sup>(1)</sup> UB=upper bound prediction, AVE=average prediction

## List of Figures

- Figure 1: Definition of critical geometric and geotechnical parameters for seismic slope stability of earth dams and tall embankments
- Figure 2: Calibration of model constants  $\alpha_1$  and  $\gamma_1$  of employed non-linear hysteretic soil model (Eqs 1 through 5) to fit the experimental curves for shear modulus  $G/G_{\max}$  degradation and hysteretic damping  $\xi$  increase with cyclic shear strain  $\gamma$  of Vucetic and Dobry (1991)
- Figure 3: Effect of height  $H$  on the elastic (first) eigen-period  $T_{oe}$  of the dam
- Figure 4: Typical numerical results for the effects of excitation characteristics (PGA and  $T_e$ ) on the dam fundamental period increase ratio ( $T_o/T_{oe}$ ) due to non-linearity
- Figure 5: Prediction accuracy of the dam fundamental period increase ratio ( $T_o/T_{oe}$ ) due to non-linearity, against all numerical data
- Figure 6: Examples of variability of dam amplification ratio  $PGA_{crest}/PGA$ , as a function of (tuning) period ratio  $T_o/T_e$  and the shear wave velocity  $V_b$  (stiffness) of the foundation soil layer
- Figure 7: Prediction accuracy of the dam amplification ratio  $PGA_{crest}/PGA$  ratio, against all numerical data
- Figure 8: Correlations of  $k_{hmax}/(PGA_{crest}/g)$  ratio with different possible expressions of the maximum depth  $z$  of the sliding mass (data from analyses with  $PGA = 0.15g$ ,  $V_b = 500m/s$ )
- Figure 9: Proposed “*fundamental*” relation of  $k_{hmax}/(PGA_{crest}/g)$  ratio versus normalized maximum depth ratio  $z/\lambda_d$ , as per Eq. (14) for  $C_1=C_b=C_f=C_g=1.0$ , against related numerical data
- Figure 10: Effect of dam reservoir on the  $k_{hmax}/(PGA_{crest}/g)$  versus  $z/\lambda_d$  relation of the upstream sliding masses on the basis of numerical data, and comparison to the “*fundamental*” relation of Eq. (14) for  $C_1=C_b=C_f=C_g=1.0$
- Figure 11: Prediction accuracy of the peak seismic coefficient  $k_{hmax}$  for sliding masses, against all numerical data
- Figure 12: Effects of important problem parameters  $T_o/T_e$ ,  $z/\lambda_d$  and  $PGA$  on the relative error of  $k_{hmax}$  prediction for all numerical data
- Figure 13: Permanent deviatoric slope displacements  $D$  as a function of  $k_y$ ,  $PGA$  and  $PGV$  from various upper bound (UB) and average (AVE) relations based on the rigid sliding block theory
- Figure 14: Correlation of sliding coefficient  $q$  to allowable displacement  $D_{all}$  and peak seismic intensity measures of the sliding mass  $k_{hmax}$  and  $v_{hmax}$  on the basis of upper bound ( $q_{UB}$ ) and average ( $q_{AVE}$ ) displacement equations
- Figure 15: Prediction accuracy of the  $(v_{hmax}/a_{hmax})$  ratio of sliding masses, against all numerical data

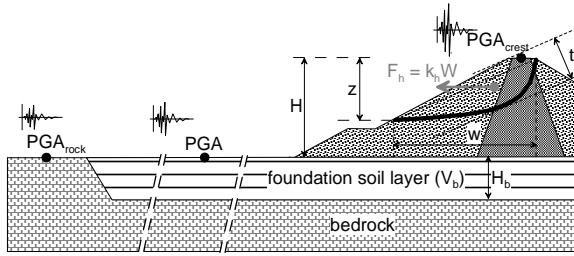


Figure 1: Definition of critical geometrical and geotechnical parameters for seismic slope stability of earth dams and tall embankments

*Single column*

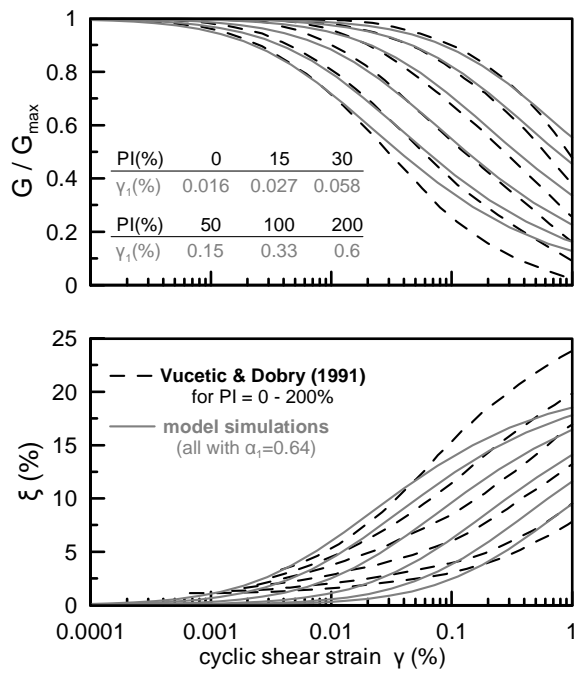


Figure 2: Calibration of model constants  $\alpha_1$  and  $\gamma_1$  of employed non-linear hysteretic soil model (Eqs 1 through 5) to fit the experimental curves for shear modulus  $G/G_{max}$  degradation and hysteretic damping  $\xi$  increase with cyclic shear strain  $\gamma$  of Vucetic and Dobry (1991)

*Single column*



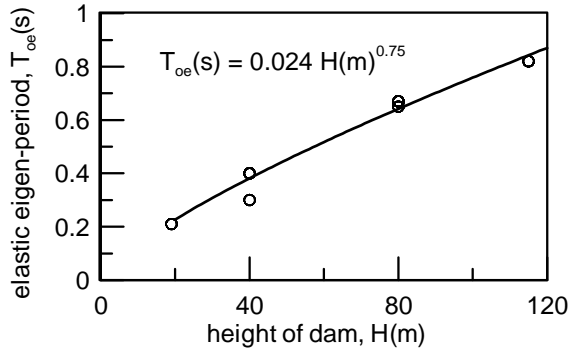


Figure 3: Effect of height  $H$  on the elastic (first) eigen-period  $T_{oe}$  of the dam

*Single column*

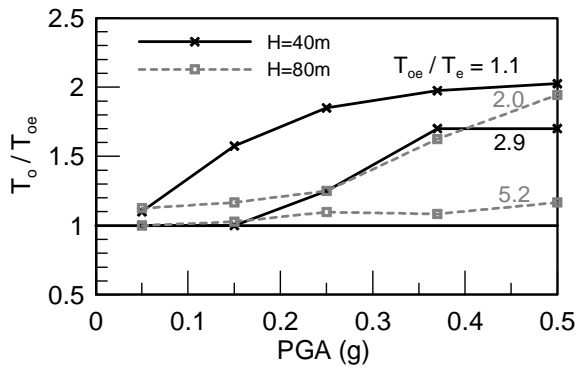


Figure 4: Typical numerical results for the effects of excitation characteristics (PGA and  $T_e$ ) on the dam fundamental period increase ratio ( $T_o/T_{oe}$ ) due to non-linearity

*Single column*

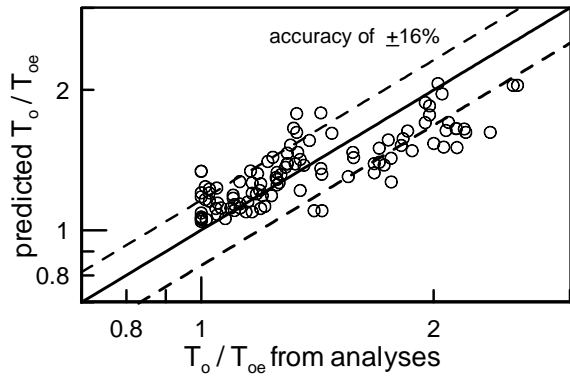


Figure 5: Prediction accuracy of the dam fundamental period increase ratio ( $T_o/T_{oe}$ ) due to non-linearity, against all numerical data

*Single column*

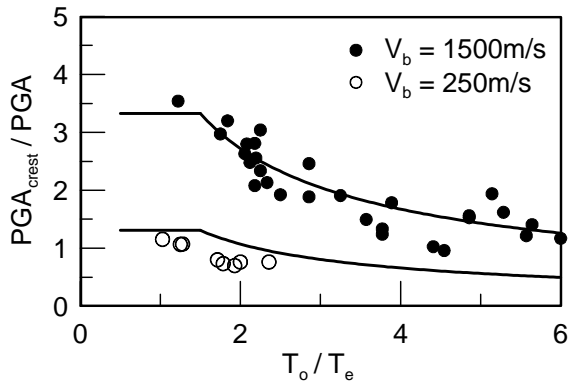


Figure 6: Examples of variability of dam amplification ratio  $PGA_{crest}/PGA$ , as a function of (tuning) period ratio  $T_o/T_e$  and the shear wave velocity  $V_b$  (stiffness) of the foundation soil layer

*Single column*

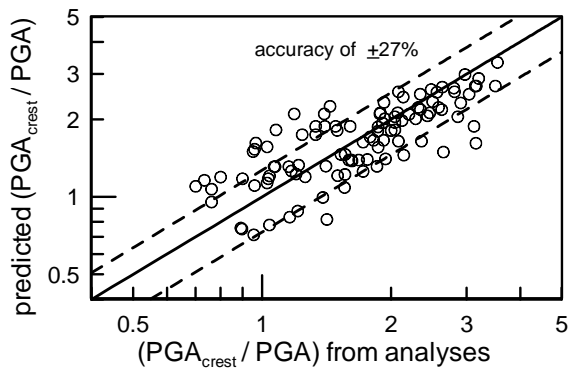


Figure 7: Prediction accuracy of the dam amplification ratio  $PGA_{crest}/PGA$  ratio, against all numerical data

*Single column*

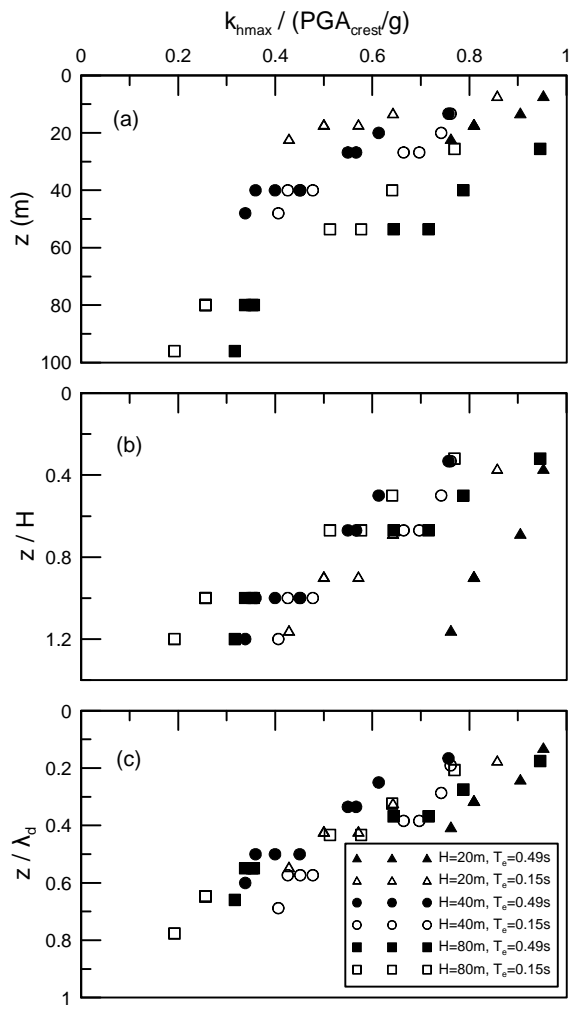


Figure 8: Correlations of  $k_{hmax} / (PGA_{crest} / g)$  ratio with different possible expressions of the maximum depth  $z$  of the sliding mass (data for  $PGA = 0.15g, V_b = 500m/s$ )

*Single column*

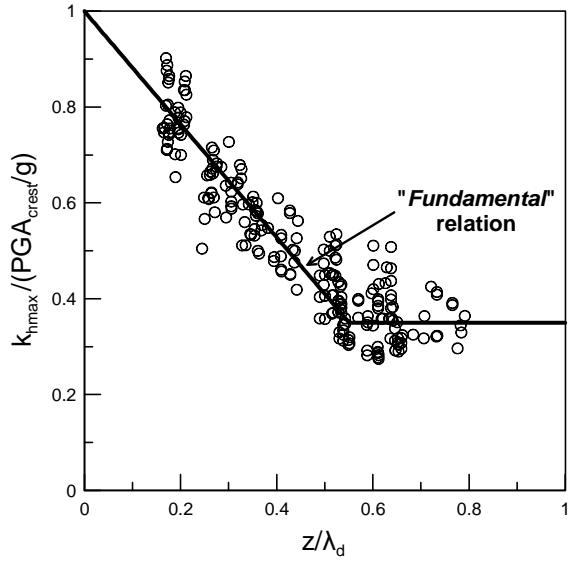


Figure 9: Proposed “*fundamental*” relation of  $k_{hmax}/(PGA_{crest}/g)$  ratio versus normalized maximum depth ratio  $z/\lambda_d$ , as per Eq. (14) for  $C_1=C_b=C_f=C_g=1.0$ , against related numerical data

*Single column*

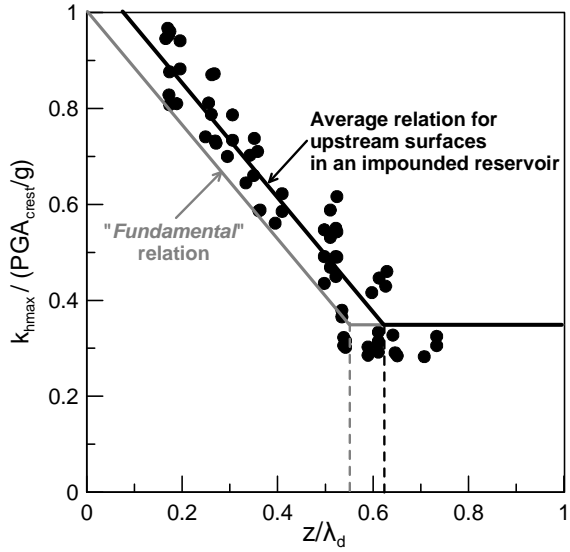


Figure 10: Effect of dam reservoir on the  $k_{hmax}/(PGA_{crest}/g)$  versus  $z/\lambda_d$  relation of the upstream sliding masses on the basis of numerical data, and comparison to the “*fundamental*” relation of Eq. (14) for  $C_1=C_b=C_f=C_g=1.0$

*Single column*

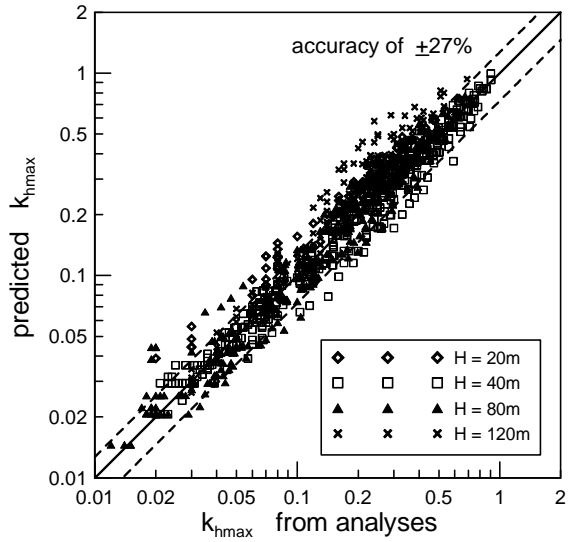


Figure 11: Prediction accuracy of the peak seismic coefficient  $k_{hmax}$  for sliding masses, against all numerical data

*Single column*

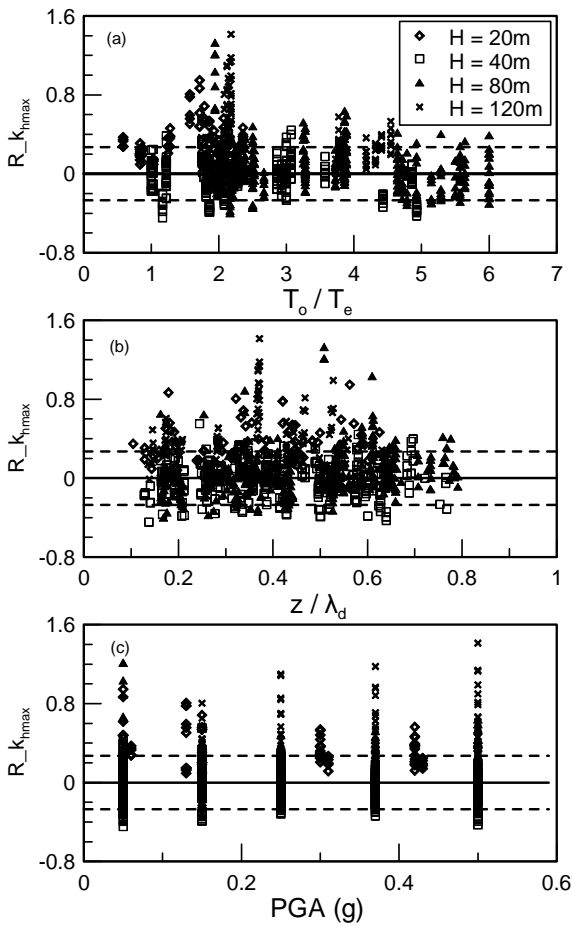


Figure 12: Effects of important problem parameters  $T_o/T_e$ ,  $z/\lambda_d$  and PGA on the relative error of  $k_{hmax}$  prediction for all numerical data

*Single column*

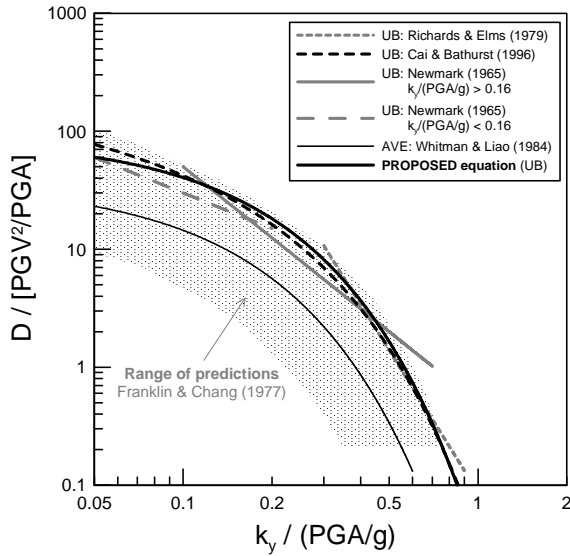


Figure 13: Permanent deviatoric slope displacements  $D$  as a function of  $k_y$ , PGA and PGV from various upper bound (UB) and average (AVE) relations based on the rigid sliding block theory

*Single column*

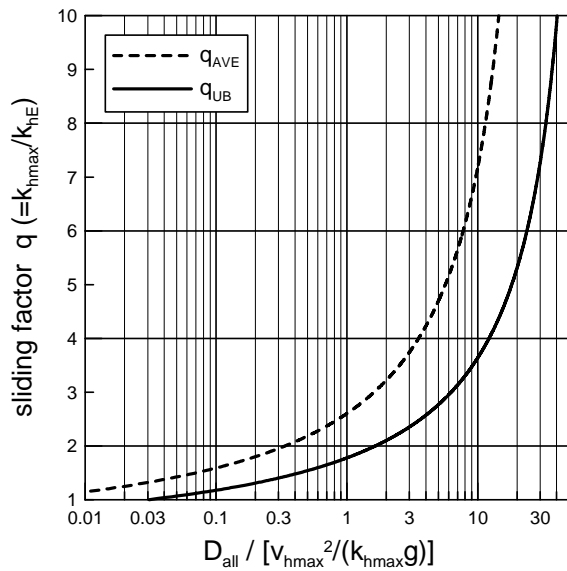


Figure 14: Correlation of sliding coefficient  $q$  to allowable displacement  $D_{all}$  and peak seismic intensity measures of the sliding mass  $k_{hmax}$  and  $v_{hmax}$  on the basis of upper bound ( $q_{UB}$ ) and average ( $q_{AVE}$ ) displacement equations

*Single column*

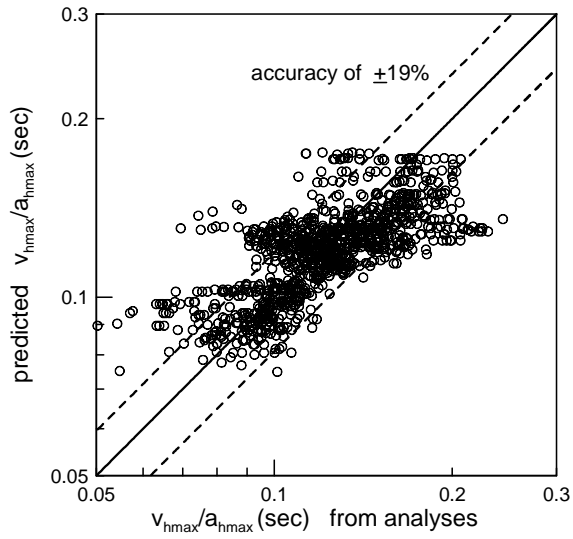


Figure 15: Prediction accuracy of the  $(v_{hmax}/a_{hmax})$  ratio of sliding masses, against all numerical data

*Single column*